Article

Research Update: Conductivity and beyond at the LaAlO$_3$/SrTiO$_3$ interface

GARIGLIO, Stefano, GABAY, M., TRISCONE, Jean-Marc

Abstract

In this review, we focus on the celebrated interface between two band insulators, LaAlO3 and SrTiO3, that was found to be conducting, superconducting, and to display a strong spin-orbit coupling. We discuss the formation of the 2-dimensional electron liquid at this interface, the particular electronic structure linked to the carrier confinement, the transport properties, and the signatures of magnetism. We then highlight distinctive characteristics of the superconducting regime, such as the electric field effect control of the carrier density, the unique tunability observed in this system, and the role of the electronic subband structure. Finally we compare the behavior of Tc versus 2D doping with the dome-like behavior of the 3D bulk superconductivity observed in doped SrTiO3. This comparison reveals surprising differences when the Tc behavior is analyzed in terms of the 3D carrier density for the interface and the bulk.

Reference

UNIVERSITÉ DE GENÈVE

Research Update: Conductivity and beyond at the LaAlO3/SrTiO3 interface

S. Gariglio, M. Gabay, and J.-M. Triscone

Research Update: Conductivity and beyond at the LaAlO₃/SrTiO₃ interface

S. Gariglio,[1,a] M. Gabay,[2] and J.-M. Triscone[1]

[1]*DQMP, University of Geneva, 24 Quai E.-Ansermet, CH-1211 Geneva, Switzerland*
[2]*Laboratoire de Physique des Solides, Université Paris-Sud, Bâtiment 510, 91405 Orsay Cedex, France*

In this review, we focus on the celebrated interface between two band insulators, LaAlO₃ and SrTiO₃, that was found to be conducting, superconducting, and to display a strong spin-orbit coupling. We discuss the formation of the 2-dimensional electron liquid at this interface, the particular electronic structure linked to the carrier confinement, the transport properties, and the signatures of magnetism. We then highlight distinctive characteristics of the superconducting regime, such as the electric field effect control of the carrier density, the unique tunability observed in this system, and the role of the electronic subband structure. Finally we compare the behavior of T_c versus 2D doping with the dome-like behavior of the 3D bulk superconductivity observed in doped SrTiO₃. This comparison reveals surprising differences when the T_c behavior is analyzed in terms of the 3D carrier density for the interface and the bulk. © *2016 Author(s). All article content, except where otherwise noted, is licensed under a Creative Commons Attribution (CC BY) license (http://creativecommons.org/licenses/by/4.0/).* [http://dx.doi.org/10.1063/1.4953822]

INTRODUCTION

Without a doubt, transition metal oxides qualify as one of the hot topics of interest as these materials are endowed with a broad range of significant electronic properties ranging from ferroelectricity to metal-insulator transitions as well as from magnetism to superconductivity. Many of these compounds exhibit structural instabilities, strong electronic correlations, and complex phase diagrams with competing ground states.[1] These features are quite desirable from an engineering perspective since they could prove instrumental in the design of novel ultrasensitive sensors with a strong response to small stimuli. Artificial structures of transition metal oxides therefore seem ideal to explore interfacial effects that could possibly lead to new phases. In this respect, the conducting layer at the interface between LaAlO₃ (LAO) and SrTiO₃ (STO) that was observed by Ohtomo and Hwang a decade ago[2] has attracted a considerable amount of attention. It was found that this two-dimensional electron liquid (2DEL) hosts gate tunable insulator to metal,[3] insulator to superconductor[4] transitions and a large interfacial spin-orbit effect.[5,6] Signatures of magnetism have also been reported in several independent studies,[7,8] underscoring the interplay between spin and charge for the electronic states. The mechanisms responsible for these features are still in debate. A significant effort has been devoted to unraveling the physics at play responsible for the formation of the 2DEL. Other key questions include the role played by the various d orbitals which could contribute selectively to a specific charge or spin property, the impact of confinement that might cause a spatial dichotomy between electrons harboring magnetic correlations and those involved in superconductivity in stark contrast with the standard behavior when all electrons participate equally in the different ground states irrespective of their position in the metallic sheet. In this brief overview, we focus on the prototypic heterostructure—LAO/STO— which has been extensively investigated worldwide and we highlight its key properties. While the interested reader may refer to
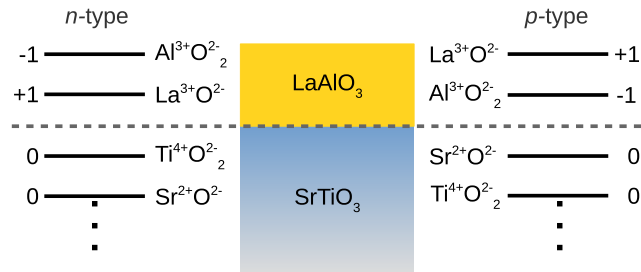
[a]Electronic address: stefano.gariglio@unige.ch

4, 060701-1

FIG. 1. Two possible interfaces can be realized: TiO_2 terminated STO-LaO (left) and SrO-terminated STO-AlO_2 (right). While the TiO_2 and SrO planes are neutral, the AlO_2 and LaO planes carry a net -1 ($|e|$) and $+1$ ($|e|$) charge per unit cell, respectively.

several excellent reviews that have been written on the subject,[9–12] we include here new findings that allow us to present a novel perspective on the superconducting state of this complex system.

THE LAO/STO SYSTEM AND THE ORIGIN OF THE TWO-DIMENSIONAL ELECTRON LIQUID

The conducting interface between the two large gap band insulators LAO and STO discovered in 2004 is today at the forefront of research on conducting interfaces. One of the key features of this fascinating system is the polar discontinuity that is found at the interface between LAO and STO.[13] As shown in Figure 1, in the [001] direction, STO alternates neutral TiO_2 and SrO planes, while for LAO, AlO_2, and LaO planes are respectively $-|e|$ and $+|e|$ (per surface unit cell) charged. The resulting polar discontinuity leads to an electric field inside the LAO layer and a potential that grows as the LAO layer thickness increases—typically by 1 V per unit cell. This is the so-called "polar catastrophe scenario" that leads to an instability as the LAO layer thickness is increased.

Polar discontinuities are not restricted to the LAO/STO system and they are found, for instance, at semiconductor GaAs/Si or GaAs/Ge interfaces.[14] There are several ways to mitigate the impact of a polar discontinuity. At GaAs/Si or GaAs/Ge interfaces, models propose that a roughening at the atomic scale solves the polar discontinuity problem.[14] At the LAO/STO interface, a 50% mixed substrate surface termination (TiO_2 and SrO) can also avert the polar catastrophe problem much in the same way as a ferroelectric breaks into domains to reduce the depolarizing field. Anti-site defects can also reduce the polar discontinuity problem.[15] In the LAO/STO case, for a TiO_2 terminated STO crystal, charge transfer from the LAO surface to the interface is an alternative way to avert the polar catastrophe. This is possible since Ti is a transition metal with different valence states.

In this latter electronic reconstruction scenario, electrons populate the $3d$ t_{2g} orbitals, implying that a fraction of the Ti^{4+} ions turns into Ti^{3+}. This mechanism takes place above a critical LAO thickness of 3 unit cells,[3] it leads to electron doping of STO and yields an n-type interface. To cancel the polar field (E_P), a charge transfer of 1/2 electron per surface unit cell is necessary, which translates into a sheet carrier density of 3.3×10^{14} cm^{-2}. For p-type (AlO_2–SrO) interfaces, the system is found to be insulating. As is often the case, an atomic reconstruction is thought to remedy the polar catastrophe in this case—2DELs are indeed rare.

Other mechanisms have been discussed—for instance La/Sr intermixing at the interface or oxygen vacancies in $SrTiO_3$.[16–19] One point worth noticing is that while such mechanisms may lead to STO doping, that is to conduction, they do not fix the polar catastrophe problem.

Recently, new models have been proposed to explain the occurrence of the electron liquid.[15,20–22] Although the polar discontinuity is still the driving force for the appearance of a conducting layer, the novelty in these approaches is that the mechanism for charge transfer is not a Zener breakdown but the formation, at the critical thickness, of oxygen vacancies on the top surface of LAO (rather than at the interface)—each neutral oxygen vacancy gives two electrons that are transferred to the interface. These models allow us to understand why the top surface is insulating and may also explain why the charge transfer is abrupt at the critical thickness.

Interesting consequences of the polar catastrophe scenario pertain to [110] and [111] oriented interfaces. For ideal, sharp boundaries the former orientation does not produce a charge discontinuity and hence is not expected to give a 2DEL while the latter has a polar discontinuity as in the [001] orientation. This can possibly impact the characteristics of the 2DEL. Experimentally, both of these interfaces are found to be conducting as discussed below.

Let us also mention that the interfacial properties of the 2D electron liquid appear to be very sensitive to the LAO top surface. Polar adsorbates, for instance, cause a change in the carrier density.[23] A metallic capping can also be used to trigger conductivity in nominally insulating 1 unit-cell thick LAO/STO samples.[24] Applying a bias to an insulating 3 unit-cell thick LAO/STO interface, by means of a back gate[3] or by using a conducting atomic force microscope (AFM) tip,[25] also produces conductivity at the interface. We discuss later how the AFM approach can be exploited to create electronic nanostructures.

REALIZATION OF CONDUCTING INTERFACES

LAO/STO interfaces are commonly prepared by pulsed laser deposition (PLD). On a TiO_2-terminated [001]-oriented $SrTiO_3$ substrate, a thin layer of $LaAlO_3$ is grown at ~800 °C in an oxygen pressure ranging from 10^{-5} to 10^{-2} mbar. Using a laser fluence of 0.5-2 J/cm^2 and 1-5 Hz repetition rate, the films grow layer-by-layer, as observed by *in situ* reflection high energy electron diffraction, reproducing the step-and-terrace surface morphology of the substrate. Figure 2 illustrates the fabrication and structural properties of LAO/STO interfaces. The effect of the oxygen pressure during (and after) the deposition has been investigated by different groups,[17–19,26] revealing the important role played by this parameter for the formation of the 2DEL. Indeed, the exposure of the STO crystal to high temperature and low oxygen pressure during the growth can result in a loss of oxygen from the substrate and substantial electron doping of the crystal. A post-deposition annealing in a high oxygen pressure (0.1-1 bar) at 500 °C before cooling down to room temperature in the same atmosphere however allows an efficient suppression of these vacancies. Molecular beam epitaxy[27] and sputtering[28] have also been successfully employed for growing conducting LAO/STO interfaces. A particularly interesting outcome of the MBE approach has been the discovery of an unexpected dependence of the 2DEL formation on the stoichiometry of the $LaAlO_3$ layer. Varying
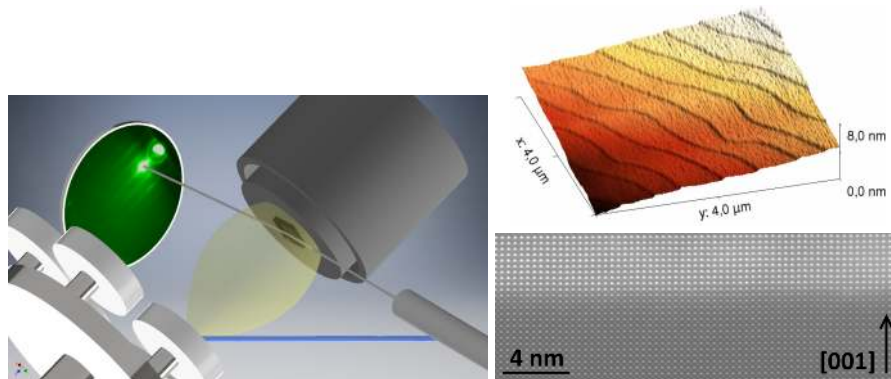
FIG. 2. Fabrication and structural properties of LAO/STO interfaces. The fabrication starts with a $SrTiO_3$ crystal cut perpendicular to the [001] direction. A chemical and thermal treatment allows a single TiO_2 termination to be obtained.[86,87] The substrate surface presents then a step-and-terrace structure due to the slight miscut off the crystallographic plane. Using pulsed laser deposition (schematized above), sputtering, or molecular beam epitaxy, an epitaxial $LaAlO_3$ layer is grown, usually a few unit cells thick. The schematic view of the PLD deposition process shows the target's carousel and sample holder. The blue line is the laser pulse producing the plume. A high energy electron beam in grazing incidence is reflected on the substrate surface and produces a diffraction pattern on a screen, also shown in the figure. In standard deposition conditions for PLD, the growth proceeds layer-by-layer, resulting in atomically smooth surfaces that reproduce the topography of the substrate (top right). Looking at the chemical contrast in a transmission electron microscope (bottom right),[88] interfaces appear atomically abrupt. For films thinner than ~20 unit cells, the epitaxial strain is preserved and a high crystalline coherence is observed.

the cationic composition of the layer, interfacial conductivity was observed only for La deficient (La/Al ratio < 0.97) films; according to this study, samples prepared by PLD are naturally La deficient (the La/Al ratio is about 0.9). This sensitivity of the 2DEL to the cation stoichiometry of the $LaAlO_3$ layer has been related to the different role of the defects (La vacancies or Al_2O_3 vacancies) in the charge transfer mechanism.

Recent work has demonstrated that 2DELs can also be formed using other crystallographic cuts of the STO substrate, opening novel possibilities for the realization of distinct electronic structures.[29,30] The origin of the 2DELs confined along these different orientations is currently investigated. In the case of [110]-oriented STO, the substrate surface is polar while the LAO/STO heterostructure does not present any polar discontinuity; for the [111]-oriented substrate, the surface is also polar but this time there is a polar discontinuity: in both cases, interfacial conductivity is observed above a critical LAO thickness, as in the (001) case. Since a crystal cannot have a polar surface that is highly unstable, these observations raise the question of the atomic configuration of the STO (110) and (111) surfaces and of the driving force behind the formation of the 2DEL for such termination planes. From a structural perspective, scanning transmission electron microscopy rules out faceting of the [110]-oriented substrate and interfaces on such planes are as sharp as in the [001] direction.[31]

Efforts to replace the two components of this interface system have been attempted with various degrees of success. The polar LAO layer has been substituted with other polar layers ($LaVO_3$,[32] $LaTiO_3$,[33] $NdGaO_3$[34]), resulting in conducting interfaces with properties similar to the LAO/STO system. Seeking for alternatives to the STO substrate has proven to be more difficult. Recent reports of interfacial conductivity in n-type LAO/ anatase TiO_2 interfaces[35]—anatase TiO_2 being structurally and electronically close to STO—and in $LaTiO_3$/$KTaO_3$[36] are promising and deserve further investigation.

ELECTRONIC PROPERTIES

The confinement of the electron liquid at the (001) interface has important consequences on the electronic structure of the 2DEL: on the one hand it produces a subband structure and determines the orbital order of the different subbands and, on the other hand, it is thought to be at the origin of the strong spin-orbit interaction observed in the system. X-ray spectroscopy has revealed that the Ti $3d - t_{2g}$ bands, which are three-fold degenerate at the Γ point for a cubic crystal, exhibit an energy splitting at the center of the Brillouin zone due to the constrained motion in the direction perpendicular to the interface: as shown in Figure 3(b), the zero point energy of states with d_{xy}-symmetry is lower than that of states with d_{xz}/d_{yz}-symmetry; the former predominantly reside in TiO_2 planes close to the interface while the latter extend further in the direction perpendicular to the interface as illustrated in Figure 3(a).[37] This particular electronic structure has been captured by *ab-initio* calculations[38,39] which also reveal that the band structure for the 2DEL is different from that of the bulk. This "interfacial" electronic structure has important consequences for the electric transport: in field effect devices, where the carrier density can be tuned with a gate voltage, the conductance was shown to change from single band to multi-band behavior upon charge filling.[40,41]

Transport at low temperature is quantitatively described by weak localisation physics, as expected for a 2D electron system. The surprise is that the Rashba spin-orbit interaction that is a common occurrence in asymmetric confining potentials, for instance in semiconductor quantum wells,[42] can be dramatically tuned by the gate voltage in LAO/STO interfaces.[5] The spin-orbit strength is found to sharply rise as the carrier density is increased and reaches very large values on the order of 10 meV. The doping range over which the spin-orbit interaction exhibits the steep increase appears to correlate with the appearance of superconductivity. Several physical interpretations of the sharp interfacial spin-orbit strength increase[5,41,43,44] have been proposed: it has been suggested that it is the change in the confinement profile induced by the electric field and related variation of the carrier density that is responsible for the modulation of the strength of the spin-orbit interaction; it could also be that the spin-orbit interaction is amplified when the Fermi level is close to an avoided crossing point—marked by a dashed line on Figure 3(c)—between electronic bands of different character. Recent experiments that show large modulations of the conduction applying the
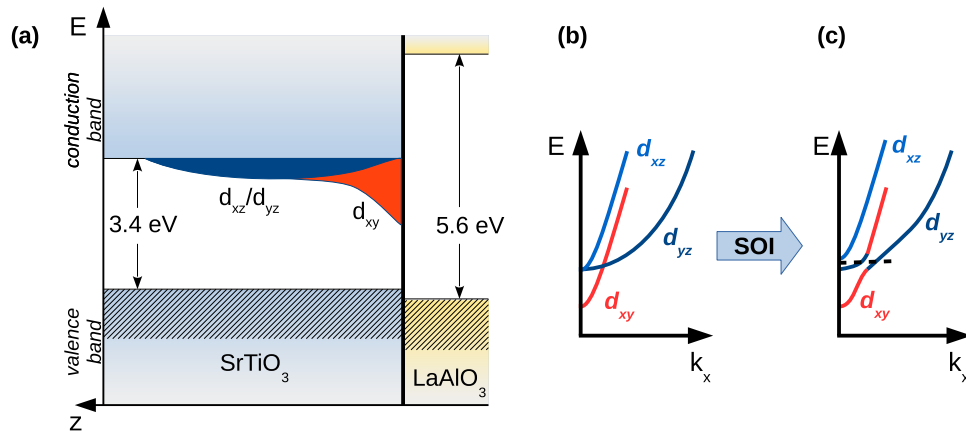
FIG. 3. Band alignment at the interface and electronic structure of the 2DEL. (a): $SrTiO_3$ and $LaAlO_3$ are two band insulators with a band gap of 3.4 eV and 5.6 eV, respectively. Once charges are transferred at the interface, they sit on the $SrTiO_3$ side in t_{2g} electronic states: the ones close to the interface are spatially localized states with d_{xy}-symmetry and extend parallel to the conduction plane; d_{xz}/d_{yz}-symmetry states extend deeper into the substrate.[89] The band alignment shown comes from *ab-initio* calculations.[9] (b) and (c): d electronic bands of the 2DEL with their different symmetries: their ordering in energy is a consequence of the hopping term perpendicular to the interface. Band structure calculations show that atomic spin-orbit interaction (SOI) and polar distortions in the TiO_2 planes due to broken inversion symmetry lift the degeneracy of d_{xz}/d_{yz}-symmetry bands causing avoided band crossings.[41,43,44] When the Fermi level (dashed line) reaches such avoided crossings, the spin-orbit interaction can be amplified.

magnetic field in plane could be satisfactorily fitted using semi-classical Boltzmann transport theory in combination with spin-orbit coupling.[45]

The spin-momentum entanglement of the charge carriers is expected to have profound consequences, beyond the ones on transport, also on magnetic and superconducting properties of the system. But, if the contribution of spin-orbit coupling to the magnetoconductance behavior is clear from the data, its impact on magnetism and superconductivity still needs to be experimentally determined as discussed below.

MAGNETISM

We just discussed the large gate tunable Rashba spin-orbit effect. We now return to this point as we review the debated experimental claims of magnetism in LAO-STO heterostructures. A search for signatures of spin-polarized states has been conducted using a variety of techniques which include magnetotransport,[46] torque[8] and SQUID magnetometry,[7] XMCD,[47,48] polarized neutron reflectometry,[49] and magnetic force microscopy.[50] Several studies concluded that a ferromagnetic alignment of magnetic moments occurs, with ordering temperatures in the range of 300 K for very low carrier concentrations (insulating limit) and of 100 K for samples that superconduct. By contrast others did not detect any fingerprint of magnetism. These clearly contradictory results raise the question of the intrinsic versus extrinsic character of the effect. In the former category, it is proposed that almost all the carriers transferred to the 2DEL during the electronic reconstruction process are localized at the interface due to disorder and/or correlations and that the residual fraction is mobile, delocalized within the conducting sheet and mediates a ferromagnetic exchange between the spins of the localized electrons. In the latter category, it is suggested that oxygen vacancies pinned near the interface are the source of the localized and extended electronic carriers in the 2DEL.[51] Both explanations contain a puzzling feature. The characteristic energy scales pertaining to the ferromagnetic state, to the Rashba spin textures, and to superconductivity are in the ballpark of a few tens of meV, a few meV a few tens of μeV, respectively. Consequently one would expect spin polarization to overpower the other states, at variance with what is reported experimentally. In an attempt to resolve this puzzle one might imagine an inhomogeneous system with magnetic patches interspersed with conducting regions. Alternative scenarios advocating an orbital selectiveness of

the d-type carrier involved in the various orderings have been proposed. These can be tested experimentally as they predict that the interplay between spin-orbit and ferromagnetism produces a spiral state albeit with a large spatial periodicity, that the superconducting state might be FFLO-like[52] and that it exhibits a Jaccarino-Peter effect.[53] At this stage it is safe to say that magnetism remains an outstanding open issue.

SUPERCONDUCTIVITY

In 2007, superconductivity was discovered at the LAO/STO interface with a critical temperature of ~250 mK.[54] Shortly after, a back gate was used to tune the carrier density.[4] Figure 4(a) displays the sheet resistance versus temperature for several gate voltages below 700 mK. As can be seen, applying an electric field allows one to switch back and forth between a zero resistance state and a resistive state at low temperature. Recording the temperature at which the resistance is reduced to 50% of its normal state value gives a widely adopted experimental mean field estimate of T_c. A typical plot of T_c versus the sheet conductance σ_{2D} is shown in Figure 4(d). Salient features of this phase diagram include a quantum critical point (QCP) separating a localized from a superconducting region at low dopings, a dome shaped curve culminating at $T_c^{max} \sim 300$ mK, a superconductor to metal boundary at higher dopings. Without gating, virgin standard samples exhibit a T_c of about 250 mK. A caveat regarding the so-called forming process is in order at this stage: before probing the interface properties for different values of V_g, one applies a positive bias V_g^{max} to the sample first; then the measured observables will not depend on the voltage sweeps, so long as $V_g < V_g^{max}$. Even so, there are sample to sample deviations in the values of T_c for a given value of V_g. If however one plots the measured transport quantity against the sheet conductance σ_{2D}, all
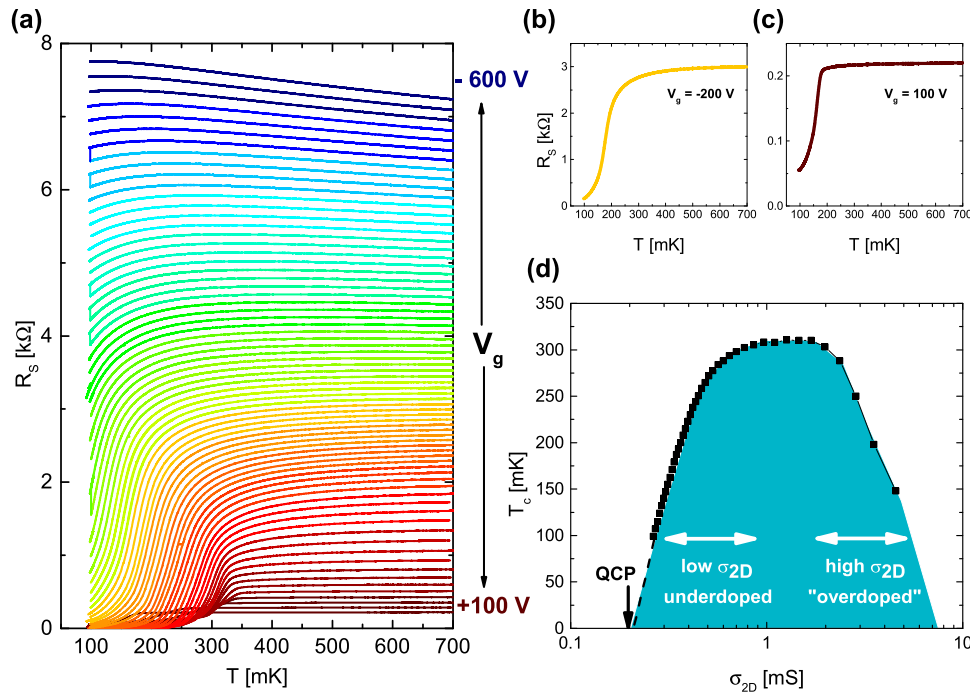
FIG. 4. Tuning of the superconducting state by field effect. In field effect devices, the carrier density can be tuned, resulting in a strong change of the transport properties. (a) Resistive superconducting transitions, sheet resistance R_S versus T, upon different gate voltages (V_g). By changing V_g the critical temperature can be reduced ("depletion" state—blue curves), reaches its maximum value close to the original doping state (red curves), and decreases again (accumulation state—brown curves). When superconductivity is suppressed for negative gate voltages, weak-localization is observed. Superconducting transitions for an underdoped (b) and an overdoped state (c). (d) Superconducting dome plotted vs the sheet conductance σ_{2D}. A criterion of 50% of the normal state resistance was used to define T_c.

curves essentially collapse on top of each other. Some of the ingredients that are likely key players in producing the characteristic shape of the phase diagram and in explaining the reproducibility issue are fluctuations, dimensionality, disorder, spin-orbit interactions. Their interplay is subtle and far from being fully understood. For instance, the rise of the spin-orbit strength that is seen upon ramping up V_g beyond the QCP correlates with the filling of the d_{xz}/d_{yz} states. These orbitals probe a significant number of unit cells of STO, making the 2DEL effectively less two-dimensional. Is the appearance of superconductivity also linked to the filling or the proximity of the d_{xz}/d_{yz} states? Not all data do agree on this point[41] and there may be a low doping superconducting regime dominated by d_{xy} states.

Dimensionality impacts the nature of the phase transition and fluctuations in its vicinity. Beyond the quantum critical point, in a doping range where the physics may still be largely dominated by the d_{xy} states, superconductivity possibly sets in through a Kosterlitz-Thouless (KT) transition. Scaling analysis of the I–V characteristics and of resistance versus T is consistent with this picture.[54] Note that spatial disorder and inhomogeneities in the normal state and superfluid densities have also been proposed as an explanation for the observed broadening of the superconducting transitions.[55,56] Measurements of the T dependence of the parallel (to the interface) critical field for the destruction of superconductivity $H_{c//}$ are in excellent agreement with a two-dimensional behavior.[57] From the determination of the perpendicular and parallel critical fields, one may extract the thickness d of the superconducting sheet. $H_{c//}$ significantly exceeds the value expected for the Pauli limit and the difference gives a measure of the strength of the spin-orbit effect when V_g is increased. In this same 2D regime, evidence of a pseudogap phase above T_c has been reported in two-point tunneling experiments.[58] This may be interpreted as a signal for the formation of uncorrelated Cooper pairs or fluctuating superconducting regions above the KT transition. The temperature where the pseudogap develops then provides an estimate of the mean field T_c. According to this picture the mean field T_c increases steadily as σ_{2D} decreases—not in line with the estimate of T_c using the 50% reduction of the resistance criterion—reaching a maximum value of about 500 mK near the QCP. Let us mention that recent measurements on quantum dots suggest pairing without phase coherence at temperature as high as 900 mK.[59] Remarkably the pseudogap line appears to merge with the superconducting boundary beyond the top of the dome, suggestive of a more three-dimensional type of transition in this region of doping. In order to test this proposal one can overlay the T$_c$ curves of LAO/STO interfaces and of bulk, oxygen reduced, STO crystals by plotting T_c/T_c^{max} versus $\sigma/\sigma(T_c^{max})$. Using dimensionless variables mitigates the difficulty in comparing changes of T_c with V_g on the one hand, with oxygen content on the other, that is, changes of T$_c$ with 2D or 3D tuning parameters, respectively.

The data (not shown) reveal that all the curves fall quite nicely on top of each other in a broad range of reduced conductivities larger than that giving T_c^{max}, indeed suggesting a more 3D behavior for the interface in this region of the phase diagram. For lower reduced conductivities deviations are observed. One still needs to clarify the influence of disorder on the phase diagram. Scaling analysis of the "zero resistance" T$_c$ versus V$_g$ near the QCP yields a critical exponent $z\nu = 2/3$ (z dynamical-, ν coherence length- critical exponents)[4] which would be expected for a clean, fermionic system. However the measured sheet resistance at the QCP is in the ballpark of 6.4 kΩ, which coincides with the value predicted by the dirty boson model.[60] A possible way to reconcile these results has been proposed by Hurand *et al.*[61] based on data analysis of LTO/STO and of LAO/STO samples.

Finally let us return to the comparison between bulk STO and the LAO/STO interface. Bulk STO can be doped by replacing Sr by La, Ti by Nb, or by reducing the oxygen content.[62–64] Superconductivity is found in a broad range of dopings as can be seen in Figure 5(a). Inspection of the data reveals that superconductivity spans several orders of magnitude in carrier density, that it appears at very low doping, a few 10^{17} cm^{-3}, and that it exhibits a dome-shape structure with a maximum T_c of about 0.3 K.

To compare doped bulk STO and LAO/STO, one has to convert the interfacial 2D sheet carrier density into a 3D one. The carrier density is not uniform and is decaying as one is moving away from the interface but, as a first step, one can simply estimate the conducting thickness d and calculate n$_{3D}$, n$_{3D}$ = n$_{2D}/d$. Close to optimum doping, for virgin samples, T_c is about 0.3 K, the
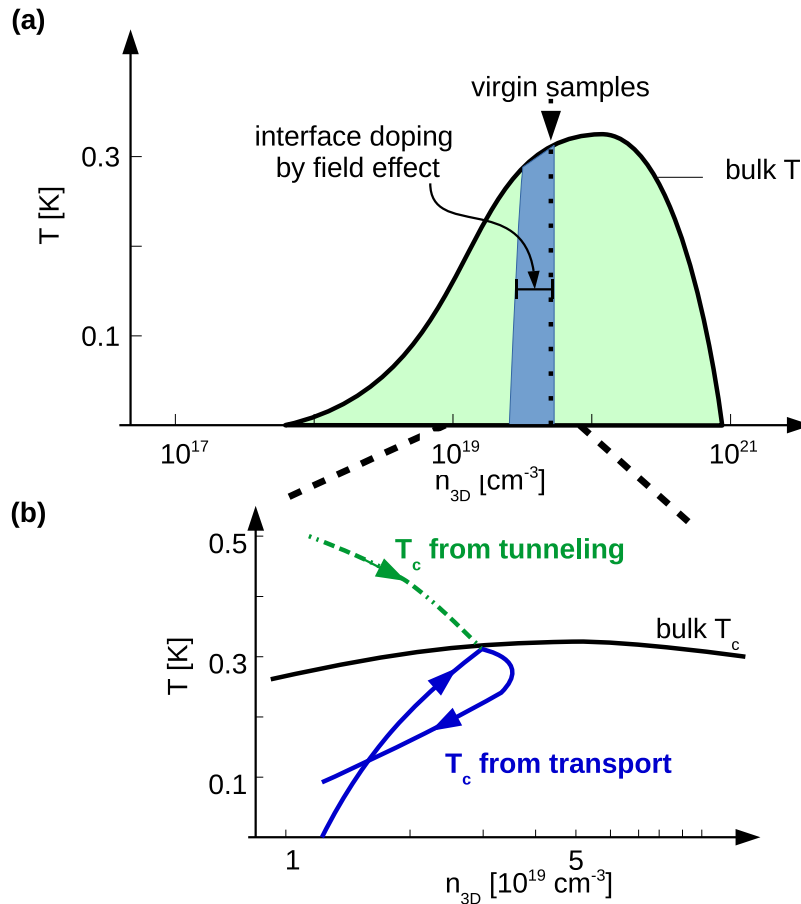
FIG. 5. Superconducting dome in bulk STO and LAO/STO interfaces. (a) Simplified behavior of T_c versus n_{3d} for bulk doped STO (black line—green area) extracted from Lin *et al.*[64] The 3D doping level of virgin samples is indicated by an arrow. The blue area is the doping range explored in the LAO/STO system while changing the gate voltage. (b) T_c versus n_{3D} for the bulk (black line) and for the LAO/STO system. The arrows indicate the behavior as one goes from the underdoped - low sheet conductance to the "overdoped" - high sheet conductance regime. Crossing the phase diagram shown in Figure 4(d), from the underdoped to the overdoped regime, is represented by the blue line. The green dashed line represents the behavior of T_c versus gate voltage or sheet conductance extracted from the tunneling data as discussed in the text.

superconducting thickness d is about 10 nm and the carrier density typically 5×10^{13} cm^{-2}, leading to $n_{3D} = 5 \times 10^{19}$ cm^{-3} (notice here that the 2D mobile carrier density is typically found to be lower than the value expected from the polar catastrophe scenario). Figure 5(a) shows that this doping, identified by an arrow, is close to that giving the maximum T_c. Field effect allows n_{2D} to be changed by a factor of 3-5 and the areal density for which the LAO/STO samples are not superconducting anymore translates into an n_{3D} around 10^{19} cm^{-3}. As can be seen in Figure 5(a), bulk STO is strongly superconducting for this value of the density. Hence, superconductivity at the interface appears at much higher doping levels than in the bulk.

This behavior may be linked to the particular interfacial band structure that we evoked previously. At the interface, using the simplified electronic structure shown in Figure 3(b), one sees that the lowest sub-bands have a d$_{xy}$ character with a low effective mass. Several of these have to be partially filled before the Fermi level reaches the energy of the heavier (higher density of states) d$_{xz}$/d$_{yz}$ sub-bands which then become occupied. By contrast, the lowest energy hybridized band in tetragonal bulk STO (taking spin-orbit into account) becomes rapidly heavy at moderate doping and hence gives rise to high density of states. From BCS theory we know that a higher density of states promotes a higher T_c. Accordingly, we may expect that for low dopings Cooper pairing is favorable in bulk STO more so than at the LAO/STO interface. Note that this scenario would naturally explain

the low superfluid density (as compared to the total mobile carrier density) observed in scanning SQUID experiments.[65] One should bear in mind the fact that we use here the superconducting thickness obtained from critical field measurements. Establishing a direct connection between this thickness, the 3D carrier density profile and the extension of the different sub-bands is far from obvious but the issue is important and definitely deserves further attention.

Recent calculations support the picture discussed above. The above scenario is also consistent with measurements of superconductivity in [110] oriented LAO/STO samples for which the orbital ordering is different from that of the [001] orientation.[66] In this case, T_c does not disappear at low doping levels.

There is an additional twist to this scenario. Very fresh experiments aimed at probing the extension of the superconducting layer across the phase diagram have revealed an unexpected behaviour of the gas confinement upon gate tuning. When extracting the superconducting thickness from $H_{c\perp}$ and $H_{c//}$ analyses, one finds that the thickness is essentially constant crossing the phase diagram from the QCP to optimal doping.[67] On the "overdoped" side, the superconducting thickness d increases by a factor of three as the doping is increased. Surprisingly, if we divide n_{2D} by d we see that n_{3D} initially increases with increasing V_g (increasing σ_{2D}) but then decreases upon further increase of V_g. n_{3D} is not a single valued function of n_{2D}, V_g, or σ_{2D} such that transport experiments only probe a limited portion of the T_c versus n_{3D} phase diagram. The peculiar T_c versus n_{3D} behavior for the interface system is shown by the blue line in Figure 5(b). This observation may be important for understanding the decrease of T_c for high conductance and has serious consequences. The magnetoconductance in the underdoped regime is very different from the one observed for the "overdoped" state.[5,40,41] n_{3D} is not an appropriate control parameter to monitor this evolution since it is not evolving monotonically but one might choose the mobility—that is increasing dramatically as one is crossing the 2D phase diagram[68]—or the sheet conductance instead. The electronic structure is directly linked to the confining potential. If the latter changes, the sub-band structure will change and we just discussed the importance of the sub-band structure for superconductivity.

The superconducting behavior that one observes for the underdoped state is quite different from the one pertaining to the "overdoped" regime except for the fact that both span a rather similar n_{3D} range. As can be seen in Figure 4(b), for negative V_g, the transition is much more rounded, a possible signature of fluctuations. As mentioned above, tunneling data show a markedly different behavior for the two doping regimes. If the correct mean field T_c is the one extracted from the gap behavior—the green dashed line in Figure 5(b)—then the connection between superconductivity and the d_{xz}/d_{yz} sub-bands would be less compelling.

To conclude this section, let us briefly return to spin-orbit and its possible influence on the superconducting state. Spin and momentum of charge carriers are entangled at the LAO/STO interface. It was mentioned above that the strength of the spin-orbit interaction increases dramatically as superconductivity develops. Such a large spin-orbit interaction—typically 10 meV—that is much larger than the superconducting gap (40 μeV) will lead to a non s-wave symmetry of the order parameter and a parallel critical field that should be substantially higher than the Pauli limit. Experimentally, a factor of three increase of the parallel critical field was observed at optimum doping with a critical field above 2 T as the Pauli limit is about 0.5-0.6 T.[57] Future experiments sensitive to the symmetry of the order parameter will allow us to better understand the interplay between spin-orbit coupling and superconductivity.

SUMMARY AND PERSPECTIVES

Since Ohtomo and Hwang's seminal discovery of conductivity at the interface between LAO and STO, numerous papers have been devoted to the field. The present review did not attempt to present a comprehensive overview on the subject, but rather to underscore three key aspects of the electronic transport in this heterostructure. One of these aspects pertains to the origin of the two-dimensional electron liquid. Different scenarios have been advocated, based on polar catastrophe, intermixing, or vacancies. We discuss the 2DEL at the (001) interface and briefly at the (110) and (111) interfaces. A second critical consideration concerns the order of the sub-bands

in the 2DEL. In bulk STO, at low temperature, the lowest band is a combination of d_{xz}/d_{yz} orbitals near the gamma point. By contrast, the lowest sub-band has a d_{xy} character in the 2DEL, a consequence of confinement. This impacts the band-filling sequence, when one gates the interface. When the d_{xz}/d_{yz} bands—which probe layers away from the interface and extend deep within the conducting sheet—start to be populated, transport evolves in a most spectacular way, as evidenced by measurements of the mobility, the interfacial spin-orbit contribution, and superconductivity. A third key aspect concerns the nature of the superconducting state that sets in when the interface is doped with electrons beyond a critical threshold. More specifically, how does it relate to the superconducting state that is observed in oxygen deficient bulk STO? We suggested that in the case of the 2DEL, Cooper pairing is established at a higher estimated 3D carrier concentration n_{3D} than in bulk STO, as a result of the "inversion" of the band filling sequence. Furthermore n_{3D} exhibits a non uniform variation with the gate voltage V_g, such that it appears to decrease upon increasing V_g beyond the top of the superconducting dome; overdoping the 2DEL is seen as increasing the oxygen content in oxygen deficient bulk STO (underdoping). Beyond these rather fundamental questions, many challenges more relating to technology issues are important. Let us mention a few of those.

High mobility is a desirable attribute of a functional device and several ideas have been successfully pursued to obtain higher mobility samples.[69–73] For instance, reducing the growth temperature[74] or using special cappings of the LAO layer[75] allows mobilities of the order of 10 000 cm^2/Vs to be reached at low temperature, these are associated with low carrier densities. The electronic structure and the control of superconductivity in such clean interfaces have yet to be determined.

Materials exhibiting giant thermopower are valuable as they may be used in the generation of electric power from thermal gradients. Very large thermopower with values of the Seebeck coefficient of up to 30 000 μV/K and giant oscillations of the Seebeck coefficient were observed as electrons were progressively removed from the LAO/STO interface.[76] The giant oscillations are understood as a signature of localized states found as the conduction band is being emptied.

Spin injection, a first step towards the fabrication of a spin field-effect transistor, has been successfully realized at the LAO/STO interface.[77,78] In these devices, spin-polarized electrons tunnel from a Co film, deposited onto the LAO layer, across the LAO tunnel barrier into the 2DEL. The spin population was probed using the Hanle effect, a measure of the junction resistance upon magnetic field sweep. A long-term goal would be to use the Rashba effect—that can itself be controlled by an electric field—to manipulate the spin of the conduction electrons along the channel between the source and the drain.

Taking advantage of the above properties for the purpose of engineering devices requires one to control the transfer of LAO/STO interfaces to other substrates. This has been tried with some success, for instance on silicon,[79] on LSAT and on NdGaO$_3$.[80] It however turned out to be difficult to preserve metallicity down to low temperatures. In multilayer structures, recent efforts have attempted to explain why these do not always lead to conducting interfaces or why only a subset of the layers is metallic. Mixed termination and the quality of the STO films seem to be the critical parameters.[81] An interesting possibility in these multilayer systems consists of coupling superconducting layers in such a way as to trigger a 2D to 3D crossover.

Last but not least, nanostructures of LAO/STO interfaces can be realized. Electron beam lithography allows one to design small channels,[82,83] and steps at STO surfaces can be used to generate nanowires.[84] The properties of such small structures have been investigated and quantum phenomena such as quantum conductance fluctuations have been observed. A very exciting and promising tool in the design of nanoscale electronic structures and circuits is the atomic force microscope (AFM) with a conducting tip. Starting from a 3 unit cell thick LAO film—that is an insulating interface—one creates conducting regions with nanometer resolution. The AFM technique is described in Figure 6. Such a technique offers the possibility to realize nanoscale electronic structures and circuits. Demonstration of nanoscale transistors and other devices has been made. This technique should allow superconducting one-dimensional wires with interesting aspect ratios to be studied as well as other fascinating mesoscopic devices.

Finally, let us mention that while the present review focuses on the LAO/STO system there are many more interesting interface systems. For instance LaTiO$_3$/STO (LTO/STO)[33] and GdTiO$_3$/STO
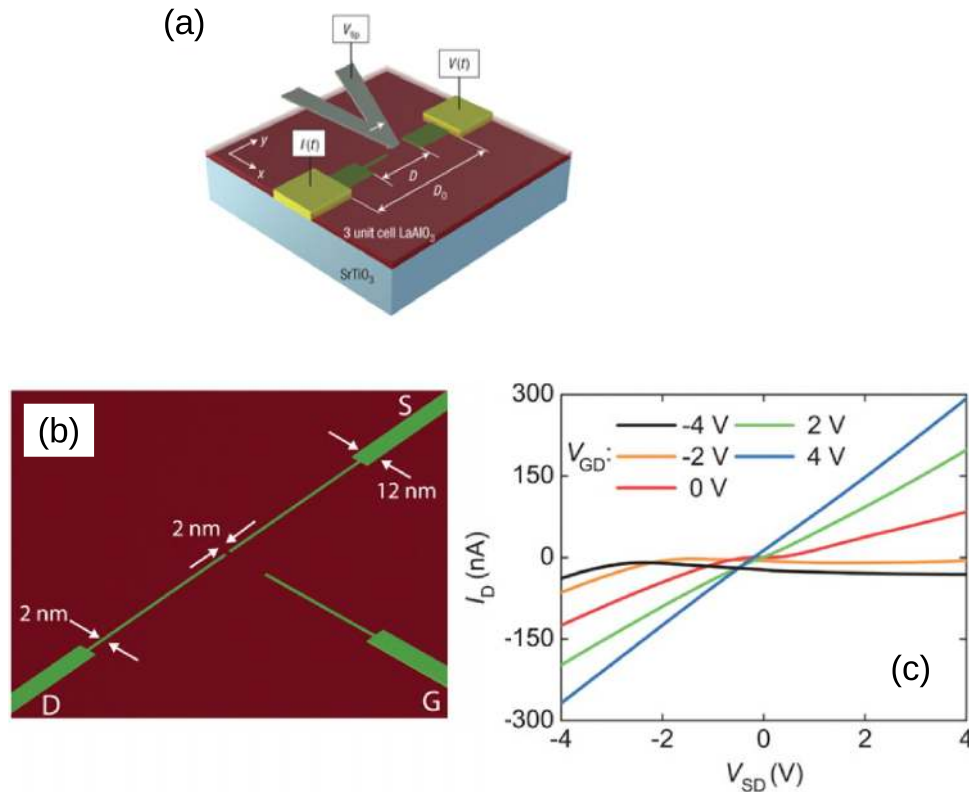
FIG. 6. AFM writing of electronic circuits. It is possible at the LAO/STO interface to use an atomic force microscopy technique to realize electronic nanostructures and circuits. The principle pioneered by the team of Jeremy Levy in Pittsburgh is based on LAO/STO samples with a LAO layer thickness of about 3 unit cells.[25] This thickness is below the threshold (4 unit cells) above which conductivity is observed. The technique uses the metallic tip of an atomic force microscope as a local source of electric field. Applying a bias between the tip and an electrode (for instance a gold layer in contact with the interface) and moving the tip away from the electrode induces locally, under the tip, a conducting area—the effect is non-volatile for some time. The width of the written conducting channel depends on the writing voltage and can be as small as a few nanometers. Panel (a) illustrates the writing process. The stability of the writing process might be linked to adsorbates that accumulate on the LAO surface while charges are transferred.[90] The process is indeed found to be sensitive to external parameters such as the humidity in the laboratory. (b) shows the design of a nanoscale transistor—a conducting path between two electrodes has been first drawn and then cut (scanning with the AFM tip perpendicular to the path and applying an opposite bias).[91] With negative bias applied to the side gate, the device is insulating (off-state) as can be seen from the drain current I_D vs source-drain voltage V_{SD} curve plotted on (c). Applying a positive voltage to the side gate allows conduction to be established, as can be seen from the linear I_D–V_{SD} curves (on-state). This technique can in principle allow the realization of complex circuits. Images taken from Refs. 25 and 91.

(GTO/STO).[85] Note that bulk LTO and GTO are Mott insulators. The LTO/STO heterostructure however displays properties very similar to those of LAO/STO. In the GTO/STO system, high mobile carrier densities are observed—corresponding to the densities expected for screening the GTO polar field—and multilayer structures with multiple conducting interfaces have been grown and studied. Several other exciting systems have been realized.[36] This flurry of novel conducting interfaces will certainly open new and interesting avenues for the investigation of low dimensional electron systems.

ACKNOWLEDGMENTS

[1] D. A. Khomskii, *Transition Metal Compounds* (Cambridge University Press, 2014).

[2] A. Ohtomo and H. Y. Hwang, "A high-mobility electron gas at the $LaAlO_3$/$SrTiO_3$ heterointerface," Nature **427**, 423–426 (2004).

[3] S. Thiel, G. Hammerl, A. Schmehl, C. W. Schneider, and J. Mannhart, "Tunable quasi-two-dimensional electron gases in oxide heterostructures," Science **313**, 1942–1945 (2006).

[4] A. D. Caviglia, S. Gariglio, N. Reyren, D. Jaccard, T. Schneider, M. Gabay, S. Thiel, G. Hammerl, J. Mannhart, and J.-M. Triscone, "Electric field control of the $LaAlO_3$/$SrTiO_3$ interface ground state," Nature **456**, 624–627 (2008).

[5] A. D. Caviglia, M. Gabay, S. Gariglio, N. Reyren, C. Cancellieri, and J.-M. Triscone, "Tunable Rashba spin-orbit interaction at oxide interfaces," Phys. Rev. Lett. **104**, 126803 (2010).

[6] M. Ben Shalom, M. Sachs, D. Rakhmilevitch, A. Palevski, and Y. Dagan, "Tuning spin-orbit coupling and superconductivity at the $SrTiO_3$/$LaAlO_3$ interface: A magnetotransport study," Phys. Rev. Lett. **104**, 126802 (2010).

[7] J. A. Bert, B. Kalisky, C. Bell, M. Kim, Y. Hikita, H. Y. Hwang, and K. A. Moler, "Direct imaging of the coexistence of ferromagnetism and superconductivity at the $LaAlO_3$/$SrTiO_3$ interface," Nat. Phys. **7**, 767–771 (2011).

[8] L. Li, C. Richter, J. Mannhart, and R. C. Ashoori, "Coexistence of magnetic order and two-dimensional superconductivity at $LaAlO_3$/$SrTiO_3$ interfaces," Nat. Phys. **7**, 762–766 (2011).

[9] R. Pentcheva and W. E. Pickett, "Electronic phenomena at complex oxide interfaces: Insights from first principles," J. Phys.: Condens. Matter **22**, 043001 (2010).

[10] P. Zubko, S. Gariglio, M. Gabay, P. Ghosez, and J.-M. Triscone, "Interface physics in complex oxide heterostructures," Annu. Rev. Condens. Matter Phys. **2**, 141–165 (2011).

[11] H. Y. Hwang, Y. Iwasa, M. Kawasaki, B. Keimer, N. Nagaosa, and Y. Tokura, "Emergent phenomena at oxide interfaces," Nat. Mater. **11**, 103–113 (2012).

[12] J. A. Sulpizio, S. Ilani, P. Irvin, and J. Levy, "Nanoscale phenomena in oxide heterostructures," Annu. Rev. Mater. Res. **44**, 117–149 (2014).

[13] N. Nakagawa, H. Y. Hwang, and D. A. Muller, "Why some interfaces cannot be sharp," Nat. Mater. **5**, 204–209 (2006).

[14] W. Harrison, E. Kraut, J. Waldrop, and R. Grant, "Polar heterojunction interfaces," Phys. Rev. B **18**, 4402–4410 (1978).

[15] L. Yu and A. Zunger, "A polarity-induced defect mechanism for conductivity and magnetism at polar-nonpolar oxide interfaces," Nat. Commun. **5**, 5118 (2014).

[16] P. Willmott, S. Pauli, R. Herger, C. Schlepütz, D. Martoccia, B. Patterson, B. Delley, R. Clarke, D. Kumah, C. Cionca, and Y. Yacoby, "Structural basis for the conducting interface between $LaAlO_3$ and $SrTiO_3$," Phys. Rev. Lett. **99**, 155502 (2007).

[17] G. Herranz, M. Basletic, M. Bibes, C. Carrétéro, E. Tafra, E. Jacquet, K. Bouzehouane, C. Deranlot, A. Hamzic, J.-M. Broto, A. Barthélémy, and A. Fert, "High mobility in $LaAlO_3$/$SrTiO_3$ heterostructures: Origin, dimensionality, and perspectives," Phys. Rev. Lett. **98**, 216803 (2007).

[18] A. Kalabukhov, R. Gunnarsson, J. Borjesson, E. Olsson, T. Claeson, and D. Winkle, "Effect of oxygen vacancies in the $SrTiO_3$ substrate on the electrical properties of the $LaAlO_3$/$SrTiO_3$ interface," Phys. Rev. B **75**, 121404 (2007).

[19] W. Siemons, G. Koster, H. Yamamoto, W. A. Harrison, G. Lucovsky, T. H. Geballe, D. H. A. Blank, and M. R. Beasley, "Origin of charge density at $LaAlO_3$ on $SrTiO_3$ heterointerfaces: Possibility of intrinsic doping," Phys. Rev. Lett. **98**(19), 196802 (2007).

[20] Z. Zhong, P. X. Xu, and P. J. Kelly, "Polarity-induced oxygen vacancies at $LaAlO_3$/$SrTiO_3$ interfaces," Phys. Rev. B **82**, 165127 (2010).

[21] Y. Li, S. N. Phattalung, S. Limpijumnong, J. Kim, and J. Yu, "Formation of oxygen vacancies and charge carriers induced in the n-type interface of a $LaAlO_3$ overlayer on $SrTiO_3$ (001)," Phys. Rev. B **84**, 245307 (2011).

[22] N. C. Bristowe, P. B. Littlewood, and E. Artacho, "Surface defects and conduction in polar oxide heterostructures," Phys. Rev. B **83**, 205405 (2011).

[23] Y. Xie, Y. Hikita, C. Bell, and H. Y. Hwang, "Control of electronic conduction at an oxide heterointerface using surface polar adsorbates," Nat. Commun. **2**, 494 (2011).

[24] E. Lesne, N. Reyren, D. Doennig, R. Mattana, H. Jaffrès, V. Cros, F. Petroff, F. Choueikani, P. Ohresser, R. Pentcheva, A. Barthélémy, and M. Bibes, "Suppression of the critical thickness threshold for conductivity at the $LaAlO_3$/$SrTiO_3$ interface," Nat. Commun. **5**, 4291 (2014).

[25] C. Cen, S. Thiel, G. Hammerl, C. W. Schneider, K. E. Andersen, C. S. Hellberg, J. Mannhart, and J. Levy, "Nanoscale control of an interfacial metal-insulator transition at room temperature," Nat. Mater. **7**, 298–302 (2008).

[26] C. Cancellieri, N. Reyren, S. Gariglio, A. D. Caviglia, A. Fête, and J.-M. Triscone, "Influence of the growth conditions on the $LaAlO_3$/$SrTiO_3$ interface electronic properties," Europhys. Lett. **91**, 17004 (2010).

[27] M. P. Warusawithana, C. Richter, J. A. Mundy, P. Roy, J. Ludwig, S. Paetel, T. Heeg, A. Pawlicki, L. F. Kourkoutis, M. Zheng, M. Lee, B. Mulcahy, W. Zander, Y. Zhu, J. Schubert, J. N. Eckstein, D. A. Muller, C. S. Hellberg, J. Mannhart, and D. G. Schlom, "$LaAlO_3$ stoichiometry is key to electron liquid formation at $LaAlO_3$/$SrTiO_3$ interfaces," Nat. Commun. **4**, 2351 (2013).

[28] J. P. Podkaminer, T. Hernandez, M. Huang, S. Ryu, C. W. Bark, S. H. Baek, J. C. Frederick, T. H. Kim, K. H. Cho, J. Levy, M. S. Rzchowski, and C. B. Eom, "Creation of a two-dimensional electron gas and conductivity switching of nanowires at the $LaAlO_3$/$SrTiO_3$ interface grown by 90° off-axis sputtering," Appl. Phys. Lett. **103**, 071604 (2013).

[29] G. Herranz, F. Sánchez, N. Dix, M. Scigaj, and J. Fontcuberta, "High mobility conduction at (110) and (111) $LaAlO_3$/$SrTiO_3$ interfaces," Sci. Rep. **2**, 758 (2012).

[30] A. Annadi, Q. Zhang, X. Renshaw Wang, N. Tuzla, K. Gopinadhan, W. M. Lü, A. Roy Barman, Z. Q. Liu, A. Srivastava, S. Saha, Y. L. Zhao, S. W. Zeng, S. Dhar, E. Olsson, B. Gu, S. Yunoki, S. Maekawa, H. Hilgenkamp, and T. Venkatesan, "Anisotropic two-dimensional electron gas at the $LaAlO_3$/$SrTiO_3$ (110) interface," Nat. Commun. **4**, 1838 (2013).

[31] D. Pesquera, M. Scigaj, P. Gargiani, A. Barla, J. Herrero-Martín, E. Pellegrin, S. M. Valvidares, J. Gázquez, M. Varela, N. Dix, J. Fontcuberta, F. Sánchez, and G. Herranz, "Two-dimensional electron gases at $LaAlO_3/SrTiO_3$ interfaces: Orbital symmetry and hierarchy engineered by crystal orientation," Phys. Rev. Lett. **113**, 156802 (2014).

[32] Y. Hotta, T. Susaki, and H. Hwang, "Polar discontinuity doping of the $LaVO_3/SrTiO_3$ interface," Phys. Rev. Lett. **99**, 236805 (2007).

[33] J. Biscaras, N. Bergeal, A. Kushwaha, T. Wolf, A. Rastogi, R. C. Budhani, and J. Lesueur, "Two-dimensional superconductivity at a Mott insulator/band insulator interface $LaTiO_3/SrTiO_3$," Nat. Commun. **1**, 89 (2010).

[34] P. Perna, D. Maccariello, M. Radovic, U. Scotti di Uccio, I. Pallecchi, M. Codda, D. Marré, C. Cantoni, J. Gazquez, M. Varela, S. J. Pennycook, and F. Miletto Granozio, "Conducting interfaces between band insulating oxides: The $LaGaO_3/SrTiO_3$ heterostructure," Appl. Phys. Lett. **97**, 152111 (2010).

[35] M. Minohara, T. Tachikawa, Y. Nakanishi, Y. Hikita, L. F. Kourkoutis, J.-S. Lee, C. Kao, M. Yoshita, H. Akiyama, C. Bell, and H. Y. Hwang, "Atomically engineered metal-insulator transition at the $TiO_2/LaAlO_3$ heterointerface," Nano Lett. **14**, 6743–6746 (2014).

[36] K. Zou, S. Ismail-Beigi, K. Kisslinger, X. Shen, D. Su, F. J. Walker, and C. H. Ahn, "$LaTiO_3/KTaO_3$ interfaces: A new two-dimensional electron gas system," APL Mater. **3**, 036104 (2015).

[37] M. Salluzzo, J. C. Cezar, N. B. Brookes, V. Bisogni, G. M. De Luca, C. Richter, S. Thiel, J. Mannhart, M. Huijben, A. Brinkman, G. Rijnders, and G. Ghiringhelli, "Orbital reconstruction and the two-dimensional electron gas at the $LaAlO_3/SrTiO_3$ interface," Phys. Rev. Lett. **102**, 166804 (2009).

[38] Z. Popović, S. Satpathy, and R. Martin, "Origin of the two-dimensional electron gas carrier density at the $LaAlO_3$ on $SrTiO_3$ interface," Phys. Rev. Lett. **101**, 256801 (2008).

[39] P. Delugas, A. Filippetti, V. Fiorentini, D. I. Bilc, D. Fontaine, and Ph. Ghosez, "Spontaneous 2-dimensional carrier confinement at the n-Type $SrTiO_3/LaAlO_3$ interface," Phys. Rev. Lett. **106**, 166807 (2011).

[40] A. Fête, S. Gariglio, A. Caviglia, J.-M. Triscone, and M. Gabay, "Rashba induced magnetoconductance oscillations in the $LaAlO_3$-$SrTiO_3$ heterostructure," Phys. Rev. B **86**, 201105 (2012).

[41] A. Joshua, S. Pecker, J. Ruhman, E. Altman, and S. Ilani, "A universal critical density underlying the physics of electrons at the $LaAlO_3/SrTiO_3$ interface," Nat. Commun. **3**, 1129 (2012).

[42] R. Winkler, *Spin-Orbit Coupling Effects in Two-Dimensional Electron and Hole Systems* (Springer, Berlin, Heidelberg, 2003).

[43] G. Khalsa, B. Lee, and A. H. Macdonald, "Theory of t_{2g} electron-gas Rashba interactions," Phys. Rev. B **88**, 041302 (2013).

[44] Z. Zhong, A. Tóth, and K. Held, "Theory of spin-orbit coupling at $LaAlO_3/SrTiO_3$ interfaces and $SrTiO_3$ surfaces," Phys. Rev. B **87**, 161102 (2013).

[45] M. Diez, A. Monteiro, G. Mattoni, E. Cobanera, T. Hyart, E. Mulazimoglu, N. Bovenzi, C. W. J. Beenakker, and A. D. Caviglia, "Giant negative magnetoresistance driven by spin-orbit coupling at the $LaAlO_3/SrTiO_3$ interface," Phys. Rev. Lett. **115**, 016803 (2015).

[46] D. A. Dikin, M. Mehta, C. W. Bark, C. M. Folkman, C. B. Eom, and V. Chandrasekhar, "Coexistence of superconductivity and ferromagnetism in two dimensions," Phys. Rev. Lett. **107**, 056802 (2011).

[47] J.-S. Lee, Y. W. Xie, H. K. Sato, C. Bell, Y. Hikita, H. Y. Hwang, and C.-C. Kao, "Titanium d_{xy} ferromagnetism at the $LaAlO_3/SrTiO_3$ interface," Nat. Mater. **12**, 703–706 (2013).

[48] M. Salluzzo, S. Gariglio, D. Stornaiuolo, V. Sessi, S. Rusponi, C. Piamonteze, G. M. De Luca, M. Minola, D. Marré, A. Gadaleta, H. Brune, F. Nolting, N. B. Brookes, and G. Ghiringhelli, "Origin of interface magnetism in $BiMnO_3/SrTiO_3$ and $LaAlO_3/SrTiO_3$ heterostructures," Phys. Rev. Lett. **111**, 087204 (2013).

[49] M. Fitzsimmons, N. Hengartner, S. Singh, M. Zhernenkov, F. Bruno, J. Santamaria, A. Brinkman, M. Huijben, H. Molegraaf, J. de la Venta, and I. Schuller, "Upper limit to magnetism in $LaAlO_3/SrTiO_3$ heterostructures," Phys. Rev. Lett. **107**, 217201 (2011).

[50] F. Bi, M. Huang, S. Ryu, H. Lee, C.-W. Bark, C.-B. Eom, P. Irvin, and J. Levy, "Room-temperature electronically-controlled ferromagnetism at the $LaAlO_3/SrTiO_3$ interface," Nat. Commun. **5**, 5019 (2014).

[51] N. Pavlenko, T. Kopp, E. Y. Tsymbal, J. Mannhart, and G. A. Sawatzky, "Oxygen vacancies at titanate interfaces: Two-dimensional magnetism and orbital reconstruction," Phys. Rev. B **86**, 064431 (2012).

[52] K. Michaeli, A. C. Potter, and P. A. Lee, "Superconducting and ferromagnetic phases in $SrTiO_3/LaAlO_3$ oxide interface structures: Possibility of finite momentum pairing," Phys. Rev. Lett. **108**, 117003 (2012).

[53] V. Jaccarino and M. Peter, "Ultra-high-field superconductivity," Phys. Rev. Lett. **9**, 290–292 (1962).

[54] N. Reyren, S. Thiel, A. D. Caviglia, L. F. Kourkoutis, G. Hammerl, C. Richter, C. W. Schneider, T. Kopp, A.-S. Rüetschi, D. Jaccard, M. Gabay, D. A. Muller, J.-M. Triscone, and J. Mannhart, "Superconducting interfaces between insulating oxides," Science **317**, 1196–1199 (2007).

[55] L. Benfatto, C. Castellani, and T. Giamarchi, "Broadening of the Berezinskii-Kosterlitz-Thouless superconducting transition by inhomogeneity and finite-size effects," Phys. Rev. B **80**, 214506 (2009).

[56] S. Caprara, M. Grilli, L. Benfatto, and C. Castellani, "Effective medium theory for superconducting layers: A systematic analysis including space correlation effects," Phys. Rev. B **84**, 014514 (2011).

[57] N. Reyren, S. Gariglio, A. D. Caviglia, D. Jaccard, T. Schneider, and J.-M. Triscone, "Anisotropy of the superconducting transport properties of the $LaAlO_3/SrTiO_3$ interface," Appl. Phys. Lett. **94**, 112506 (2009).

[58] C. Richter, H. Boschker, W. Dietsche, E. Fillis-Tsirakis, R. Jany, F. Loder, L. F. Kourkoutis, D. A. Muller, J. R. Kirtley, C. W. Schneider, and J. Mannhart, "Interface superconductor with gap behaviour like a high-temperature superconductor," Nature **502**, 528–531 (2013).

[59] G. Cheng, M. Tomczyk, S. Lu, J. P. Veazey, M. Huang, P. Irvin, S. Ryu, H. Lee, C.-B. Eom, C. S. Hellberg, and J. Levy, "Electron pairing without superconductivity," Nature **521**, 196–199 (2015).

[60] M. P. A. Fisher and G. Grinstein, "Quantum critical phenomena in charged superconductors," Phys. Rev. Lett. **60**, 208–211 (1988).

[61] S. Hurand, J. Biscaras, N. Bergeal, C. Feuillet-Palma, G. Singh, A. Jouan, A. Rastogi, A. Dogra, P. Kumar, R. C. Budhani, N. Scopigno, S. Caprara, M. Grilli, and J. Lesueur, "Density driven fluctuations in a two-dimensional superconductor," e-print arXiv:1506:06874 (2015).

[62] J. Schooley, W. Hosler, E. Ambler, J. Becker, M. Cohen, and C. Koonce, "Dependence of the superconducting transition temperature on carrier concentration in semiconducting SrTiO$_3$," Phys. Rev. Lett. **14**, 305–307 (1965).

[63] C. S. Koonce, M. L. Cohen, J. Schooley, W. R. Hosler, and E. R. Pfeiffer, "Superconducting transition temperatures of semiconducting SrTiO$_3$," Phys. Rev. **163**, 380 (1967).

[64] X. Lin, G. Bridoux, A. Gourgout, G. Seyfarth, S. Krämer, M. Nardone, B. Fauqué, and K. Behnia, "Critical doping for the onset of a two-band superconducting ground state in SrTiO$_{3-\delta}$," Phys. Rev. Lett. **112**, 207002 (2014).

[65] J. Bert, K. Nowack, B. Kalisky, H. Noad, J. Kirtley, C. Bell, H. Sato, M. Hosoda, Y. Hikita, H. Hwang, and K. Moler, "Gate-tuned superfluid density at the superconducting LaAlO$_3$/SrTiO$_3$ interface," Phys. Rev. B **86**, 060503 (2012).

[66] G. Herranz, G. Singh, N. Bergeal, A. Jouan, J. Lesueur, J. Gázquez, M. Varela, M. Scigaj, N. Dix, F. Sánchez, and J. Fontcuberta, "Engineering two-dimensional superconductivity and Rashba spin–orbit coupling in LaAlO$_3$/SrTiO$_3$ quantum wells by selective orbital occupancy," Nat. Commun. **6**, 6028 (2015).

[67] A. Fête, S. Gariglio, and J.-M. Triscone (unpublished).

[68] C. Bell, S. Harashima, Y. Kozuka, M. Kim, B. G. Kim, Y. Hikita, and H. Y. Hwang, "Dominant mobility modulation by the electric field effect at the LaAlO$_3$/SrTiO$_3$ interface," Phys. Rev. Lett. **103**, 226802 (2009).

[69] A. D. Caviglia, S. Gariglio, C. Cancellieri, B. Sacépé, A. Fête, N. Reyren, M. Gabay, A. F. Morpurgo, and J.-M. Triscone, "Two-dimensional quantum oscillations of the conductance at LaAlO$_3$/SrTiO$_3$ interfaces," Phys. Rev. Lett. **105**, 236802 (2010).

[70] M. Ben Shalom, A. Ron, A. Palevski, and Y. Dagan, "Shubnikov-de Haas oscillations in SrTiO$_3$/LaAlO$_3$ interface," Phys. Rev. Lett. **105**, 206401 (2010).

[71] A. Fête, S. Gariglio, C. Berthod, D. Li, D. Stornaiuolo, M. Gabay, and J. M. Triscone, "Large modulation of the Shubnikov-de Haas oscillations by the Rashba interaction at the LaAlO$_3$/SrTiO$_3$ interface," New J. Phys. **16**, 112002 (2014).

[72] Y. Xie, C. Bell, M. Kim, H. Inoue, Y. Hikita, and H. Y. Hwang, "Quantum longitudinal and Hall transport at the LaAlO$_3$/SrTiO$_3$ interface at low electron densities," Solid State Commun. **197**, 25–29 (2014).

[73] Y. Z. Chen, F. Trier, T. Wijnands, R. J. Green, N. Gauquelin, R. Egoavil, D. V. Christensen, G. Koster, M. Huijben, N. Bovet, S. Macke, F. He, R. Sutarto, N. H. Andersen, J. A. Sulpizio, M. Honig, G. E. D. K. Prawiroatmodjo, T. S. Jespersen, S. Linderoth, S. Ilani, J. Verbeeck, G. Van Tendeloo, G. Rijnders, G. A. Sawatzky, and N. Pryds, "Extreme mobility enhancement of two-dimensional electron gases at oxide interfaces by charge-transfer-induced modulation doping," Nat. Mater. **14**, 801–806 (2015).

[74] A. Fête, C. Cancellieri, D. Li, D. Stornaiuolo, A. D. Caviglia, S. Gariglio, and J.-M. Triscone, "Growth-induced electron mobility enhancement at the LaAlO$_3$/SrTiO$_3$ interface," Appl. Phys. Lett. **106**, 051604 (2015).

[75] A. McCollam, S. Wenderich, M. K. Kruize, V. K. Guduru, H. J. A. Molegraaf, M. Huijben, G. Koster, D. H. A. Blank, G. Rijnders, A. Brinkman, H. Hilgenkamp, U. Zeitler, and J. C. Maan, "Quantum oscillations and subband properties of the two-dimensional electron gas at the LaAlO$_3$/SrTiO$_3$ interface," APL Mater. **2**, 022102 (2014).

[76] I. Pallecchi, F. Telesio, D. Li, A. Fête, S. Gariglio, J.-M. Triscone, A. Filippetti, P. Delugas, V. Fiorentini, and D. Marré, "Giant oscillating thermopower at oxide interfaces," Nat. Commun. **6**, 6678 (2015).

[77] N. Reyren, M. Bibes, E. Lesne, J. M. George, C. Deranlot, S. Collin, A. Barthélémy, and H. Jaffrès, "Gate-controlled spin injection at LaAlO$_3$/SrTiO$_3$ interfaces," Phys. Rev. Lett. **108**, 186802 (2012).

[78] A. G. Swartz, S. Harashima, Y. Xie, D. Lu, B. Kim, C. Bell, Y. Hikita, and H. Y. Hwang, "Spin-dependent transport across Co/LaAlO$_3$/SrTiO$_3$ heterojunctions," Appl. Phys. Lett. **105**, 032406 (2014).

[79] J. W. Park, D. F. Bogorin, C. Cen, D. A. Felker, Y. Zhang, C. T. Nelson, C. W. Bark, C. M. Folkman, X. Q. Pan, M. S. Rzchowski, J. Levy, and C. B. Eom, "Creation of a two-dimensional electron gas at an oxide interface on silicon," Nat. Commun. **1**, 94 (2010).

[80] C. W. Bark, D. a. Felker, Y. Wang, Y. Zhang, H. W. Jang, C. M. Folkman, J. W. Park, S. H. Baek, H. Zhou, D. D. Fong, X. Q. Pan, E. Y. Tsymbal, M. S. Rzchowski, and C. B. Eom, "Tailoring a two-dimensional electron gas at the LaAlO$_3$/SrTiO$_3$ (001) interface by epitaxial strain," Proc. Natl. Acad. Sci. U. S. A. **108**, 4720–4724 (2011).

[81] D. Li, S. Gariglio, C. Cancellieri, A. Fête, D. Stornaiuolo, and J.-M. Triscone, "Fabricating superconducting interfaces between artificially grown LaAlO$_3$ and SrTiO$_3$ thin films," APL Mater. **2**, 012102 (2014).

[82] D. Stornaiuolo, S. Gariglio, N. J. G. Couto, A. Fête, A. D. Caviglia, G. Seyfarth, D. Jaccard, A. F. Morpurgo, and J.-M. Triscone, "In-plane electronic confinement in superconducting LaAlO$_3$/SrTiO$_3$ nanostructures," Appl. Phys. Lett. **101**, 222601 (2012).

[83] P. P. Aurino, A. Kalabukhov, N. Tuzla, E. Olsson, T. Claeson, and D. Winkler, "Nano-patterning of the electron gas at the LaAlO$_3$/SrTiO$_3$ interface using low-energy ion beam irradiation," Appl. Phys. Lett. **102**, 201610 (2013).

[84] A. Ron and Y. Dagan, "One-dimensional quantum wire formed at the boundary between two insulating LaAlO$_3$/SrTiO$_3$ interfaces," Phys. Rev. Lett. **112**, 136801 (2014).

[85] P. Moetakef, T. A. Cain, D. G. Ouellette, J. Y. Zhang, D. O. Klenov, A. Janotti, C. G. Van de Walle, S. Rajan, S. J. Allen, and S. Stemmer, "Electrostatic carrier doping of GdTiO$_3$/SrTiO$_3$ interfaces," Appl. Phys. Lett. **99**, 232116 (2011).

[86] M. Kawasaki, K. Takahashi, T. Maeda, R. Tsuchiya, M. Shinohara, O. Ishiyama, T. Yonezawa, M. Yoshimoto, and H. Koinuma, "Atomic control of the SrTiO$_3$ crystal surface," Science **266**, 1540–1542 (1994).

[87] G. Koster, B. L. Kropman, G. J. H. M. Rijnders, D. H. A. Blank, and H. Rogalla, "Quasi-ideal strontium titanate crystal surfaces through formation of strontium hydroxide," Appl. Phys. Lett. **73**, 2920–2922 (1998).

[88] The transmission electron microscope image was taken by G. Tieri, A. Gloter and O. Stéphan at LPS, Université Paris-Sud.

[89] S. Gariglio, A. Fête, and J.-M. Triscone, "Electron confinement at the LaAlO$_3$/SrTiO$_3$ interface," J. Phys.: Condens. Matter **27**, 283201 (2015).

[90] F. Bi, D. F. Bogorin, C. Cen, C. W. Bark, J. W. Park, C. B. Eom, and J. Levy, "'Water-cycle' mechanism for writing and erasing nanostructures at the LaAlO$_3$/SrTiO$_3$ interface," Appl. Phys. Lett. **97**, 173110 (2010).

[91] C. Cen, S. Thiel, J. Mannhart, and J. Levy, "Oxide nanoelectronics on demand," Science **323**, 1026–1030 (2009).